Catalysis Today 169 (2011) 167–174

Contents lists available at ScienceDirect

Catalysis Today

journal homepage: www.elsevier.com/locate/cattod

SBA-15 as a support for palladium in the direct synthesis of H_2O_2 from H_2 and O_2

S. Abate, P. Lanzafame, S. Perathoner, G. Centi*

Dipartimento di Chimica Industriale ed Ingegneria dei Materiali and INSTM – CASPE, University of Messina, V.le F. Stagno D'Alcontres 31, 98166 Messina, Italy

ARTICLE INFO

Article history:
Available online 18 November 2010

Dedicated to the memory of professor Jerzy Haber which will continue to enlighten us for his pivotal contribution to both fundamental and applied advances in catalysis science.

Keywords:
H_2O_2 direct synthesis
Pd–SBA-15
CO_2-expanded methanol
Palladium

ABSTRACT

The behavior of a catalyst prepared by deposition of Pd nanoparticles over a mesoporous SBA-15 support is compared with that of Pd supported over commercial silica in the direct synthesis of H_2O_2 from H_2 and O_2. The activity was studied in a batch and semi-batch autoclave operating at r.t. and at pressures of 6.5 bar using methanol as the solvent in the presence or absence of CO_2. The use of CO_2-expanded methanol leads to a significant increase in the rate of H_2O_2 synthesis of both Pd–SiO_2 and Pd–SBA-15 samples, especially in the latter. The effect derives from an increased solubility of H_2 and O_2 which increases the reaction rate, but also determines a relocation of Pd particles which migrate inside the mesopore channels of SBA-15. For the longer times of reaction, elongated Pd particles form which probably partially inhibit the reactant diffusion. This determines a decrease of the productivity which, however, at the maximum is about 2.5 times higher than that of the analogous Pd–SiO_2 sample in semi-batch continuous tests. The use of CO_2-expanded methanol leads also to an enhanced rate of H_2O_2 decomposition, particularly in Pd–SBA-15 sample where together with the H_2O_2 hydrogenolysis an additional path due to H_2O_2 decomposition catalyzed by weak acid groups (silanols) is present. The addition of pyridine to the solution strongly inhibits both reactions, but also the synthesis of H_2O_2 due probably to the strong chemisorption over the Pd particles. The grafting with Ti of the inner walls of SBA-15 channels to decrease the amount of silanol groups has a positive effect to control the decomposition of H_2O_2 catalyzed by these groups.

1. Introduction

The start of operations of new large scale processes using H_2O_2 as reactant (synthesis of caprolactam by Sumitomo and propene oxide by DSM/BASF) [1,2], the interest of other companies in new processes based on the use of H_2O_2 as the oxidation (direct phenol synthesis from benzene, catalytic epoxidation and hydroxylation for the synthesis of intermediate and fine chemicals) [3] and the expansion of the use of H_2O_2 in pulp and paper bleaching, municipal and industrial water treatment, textile treatment, sodium percarbonate for detergents, etc. have turned again positive the outlooks for a significant expansion of the H_2O_2 market starting from the year 2010 after the negative trend in years 2008–2009 due to the general economic crisis. This has also further stimulated the research interest on the direct synthesis of H_2O_2 from H_2 and O_2 [4–6] which has some potential advantages over the commercial alkylanthraquinone route in terms of simpler operations and reduced environmental impact, although it has major drawbacks deriving from the need to operate with diluted H_2 and O_2 gaseous feeds to be outside the explosion range of the O_2/H_2/inert mixture, with the consequence of low productivities, which imply the need of high pressure operations (ca. 100 bar).

Several papers have been published recently on the catalysts for the direct synthesis of H_2O_2. Most of the studies focused on the modification of the properties of Pd by alloying/doping with a second metal (Au, Pt). For example, Menegazzo et al. [7] pointed out that the effect of the addition of gold to Pd in enhancing the yield of H_2O_2 is sensitive to the preparation method, due to the multiple role of Au in changing the chemical composition of the metallic particles, their morphology and charge of the exposed Pd sites. Also Pt, even if only at much lower levels of doping [8] as reported in many patents [5], has a positive effect on the performances of Pd, suggesting that the key role of the second metal is a modification of the morphological characteristics of Pd particles more than an electronic effect, although Liu et al. [9] gave an opposite interpretation. The effect of Au is generally associated to the blocking of the sites for the decomposition of H_2O_2 [10–16]. Theoretical studies suggest that a mechanism based on the reaction of the superoxo precursor state of the dioxygen molecule on Pd surface with two hydrogen atoms situated over neighboring 3-fold positions [15]. The competitive reaction of dioxygen dissociation leading to the nonselective formation of water is blocked by the presence of surface gold atoms. Ham et al. [16] studying by periodic DFT method Pd ensembles, demonstrated that H_2O_2 formation is strongly affected by the spatial arrangement of Pd and Au surface atoms. Pd monomers surrounded by less active Au atoms that suppress O–O bond scission are primarily responsible for the significantly enhanced selectivity toward H_2O_2 formation on Pd–Au alloys compared to that on the monometallic Pd and Au counterparts.

---

* Corresponding author.
E-mail address: centi@unime.it (G. Centi).

0920-5861/$ – see front matter © 2010 Elsevier B.V. All rights reserved.
doi:10.1016/j.cattod.2010.09.030

A second group of papers were instead focused on the role of the support in the modification of properties of supported Pd particles. One common observation in patents and fundamental studies is that an acidic support promotes the selectivity. Among the solid acids used for the direct synthesis of H_2O_2 should be mentioned zirconia [17] and sulfated zirconia [18], fluorinated alumina [19], Keggin-type polyoxometalate [20], silica [21] and sulfonic acid-functionalized silica [22], graphite [23] and active carbon [24], functionalized carbons with sulfonic acid groups or sulfonic acid functionalized polystyrene resins (PS–SO_3H) [25,26], N-doped carbon nanotubes [27], TiO_2 [12], TS-1 [28,29], Ti–MCM-41 [30], etc. The results reported in literature underline that the catalytic performance of the catalyst is strongly affected by the characteristics of the support, but that it is still unclear what the best type of support is. The different research groups have different claims regarding the best type of support, but the results are often not easy comparable due to the different type of reaction conditions and experimentations.

The problem lies in the fact that the reaction network in H_2O_2 synthesis and decomposition is complex, with the presence of parallel and secondary reactions which affect the selectivity [31], the readsorption of H_2O_2 and the hydrolysis catalyzed either by basic or acid sites is an important aspect in relation to the effect of the support, but which in turn also influence the specific nature of the Pd particles. In addition, the catalytic performances depend on the state of Pd during the catalytic reaction, e.g. metallic Pd or PdO (and all the possible intermediate situations, such as metallic Pd with sub-surface oxygen, a PdO layer on a core of metallic Pd or the contrary, etc.) [21,32,33]. The effective state of Pd particles during the catalytic reaction in turn strongly depend on the reaction conditions, e.g. the type of solvent, the H_2:O_2 ratio in the feed, the addition of modifier in solution (halides or sulfuric acids are the most common), etc. [34]. Few studies have been dedicated to the analysis of the effect of the reaction conditions on the catalytic performances in H_2O_2 synthesis and even much less on the identification of how the optimal catalyst characteristics depend on the reaction conditions.

We earlier shortly reported that the use of CO_2-expanded methanol has a significant effect in improving the catalytic performances in the direct synthesis of H_2O_2, possibly due to an enhanced solubility of O_2 in the reaction medium [3,35]. Other authors found also that CO_2 under supercritical conditions promotes the performances in the direct synthesis of H_2O_2 [7,36]. We also suggested that the use of mesoporous materials could synergistically further promote the behavior, due to a confinement effect inside the channels.

While the use of different supports for Pd particles has been extensively investigated, mesoporous materials have received limited attention. They show potentially two interesting characteristics. The first is related to the possible high dispersion and stabilization of Pd particles inside the mesoporous channels. The second is related to the possible presence of confinement effects, e.g. a modification of fluid characteristics due to the wall effect in nanoscale channels.

We have thus investigated the performances of Pd–SBA-15 catalysts, with respect to those of analogous samples prepared using commercial silica, in the synthesis and decomposition of H_2O_2 using CO_2-expanded methanol as the solvent. The aim is to give a further contribution to the understanding of the nature of the active catalysts in relation to the reaction conditions.

2. Experimental

2.1. Preparation of the catalysts

As the support for deposition of Pd by incipient wetness method the following materials were used: commercial SiO_2, and home-made SBA-15 and Ti–SBA-15 (a SBA-15 sample modified post-synthesis by grafting Ti to have a reconstruction of the corona area – e.g. of microporous regions inside the SBA-15 channels [37]. These samples will be indicated hereinafter as *Pd–SiO₂*, *Pd–SBA* and *Pd–Ti–SBA*.

Commercial silica was obtained from PQ Corporation (MS-3030) and has a surface area of 300–320 m^2/g. SBA-15 was synthetized with a modification of the procedure described by Zhao et al. [38] using self-assembling on Pluronic P123 triblock polymer (PEO–PPO–PEO, Aldrich). Twenty grams of PEO–PPO–PEO were dissolved in a mixture of 465 g distilled water and 130 g hydrochloric acid (HCl 37%) and stirred for 30 min at room temperature. Forty grams of tetraethyl orthosilicate (TEOS) were added to this polymer solution under vigorous magnetic stirring. The resulting gel mixture was stirred for 20 h at 35 °C and then heated for 21 h at 90 °C. The solid product was filtered and dried for 6 h at 80 °C in an oven. The product was then slurred in ethanol under reflux condition in order to remove the polymer, filtered and washed with ethanol and dried at 100 °C for 48 h. The white product was calcined at 500 °C for 6 h. The grafting of titanium on SBA-15 was realized following this procedure: titanium isopropoxide ($Ti(OPr)_4$, in an amount to have a Si/Ti ratio of 0.1) was dissolved with 20 ml of anhydrous ethanol. 150 ml of the same solvent used to solubilize titanium isopropoxide was put in a batch well stirred reactor maintained under nitrogen atmosphere. SBA-15 (1–2 g), pretreated at 140 °C, 12 h) in order to remove the adsorbed water, was added to this solution under continuous stirring. Then, titanium isopropoxide/organic solvent solution was slowly added. After completing the addition of the titanium solution, the reactor was maintained under stirring overnight at room temperature. The BET surface area of SBA-15 sample was 664 m^2/g, while that of Ti–SBA-15 sample 586 m^2/g (10.8 wt.% the amount of TiO_2). Further details on the preparation and the samples characterization were reported elsewhere [37,39].

Palladium was deposited over these supports by incipient wetness method: a solution (ca. 20 ml) of HCl 0.01 M and $PdCl_2$ (Sigma–Aldrich) precursor was added drop-wise to the supports (SiO_2, SBA-15) under stirring up to complete filling of the pore volume. Then the sample was dried in air at 120 °C overnight slowly increasing the temperature (2 °C/min). The samples were then calcined at 500 °C in air.

2.2. Characterization of the catalysts

The wt.% of the metal incorporated into the support after the preparation and after the catalytic tests, as well as the amount of leached Pd in solution during the catalytic tests, were determined by atomic absorption spectroscopy (AA) using a Perkin-Elmer Analyst 200 instrument. Samples for analysis were prepared dissolving 20 mg of the dried catalyst in an aqua regia solution. The amount of Pd (wt.%) in the samples was the following: 3.6% (Pd–SiO_2), 4.4% (Pd–SBA) and 5.0% (Pd–Ti–SBA).

Surface areas were obtained from N_2-adsorption–desorption isotherms using BET method. The samples were outgassed under vacuum at 100 °C for 5 h. Isotherms were obtained at the temperature of liquid nitrogen using a Micrometrics ASAP 2010 system. X-ray diffraction (XRD) patterns were recorded on an Ital-Structures XRD diffractometer using Cu Kα radiation (k = 1.5405 Å). The data were collected from 0.8° to 4° (2 h) with a resolution of 0.02° (small-angle X-ray scattering, SAXS) or in the 10–80° (2 h) with a resolution of 0.1° (conventional wide-angle XRD patterns). Transmission electron microscopy (TEM) studies were made on a Philips CM200 TEM FEG. The samples were dry-deposited on a holey carbon film supported on a Cu grids.

2.3. Catalytic test

The catalysts were tested in the catalytic oxidation of H_2 to H_2O_2 at 20 °C in a stirred steel reactor coated with Teflon (capacity 300 ml), containing 200 mg of catalyst in a fine powder form and 150 ml of anhydrous CH_3OH as a reaction medium with 150 μl of H_2SO_4 as promoter. A gas mixture containing H_2 and O_2 with a H_2/O_2 ratio of 1:2, CO_2 and N_2 was bubbled continuously through the reaction medium at room temperature until the pressure reached the set value of 6.5 bar. After reaching this pressure, the feed was stopped and stirring (1300 rpm) started following the progress of the reaction for 4 h. This procedure for the catalytic tests was indicated as *batch reactor* tests hereinafter. During the reaction, the total pressure decreased from the initial value of 6.5 bar to about 4.5–5.0 bar (depending on the catalyst activity) in the first hour to decrease then slowly up to 4.2–4.5 bar in the further 3 h of reaction.

A modification of this procedure was indicated as *semi-batch continuous tests*. In this case, the feed was continuously sent to the autoclave in order to maintain constant the pressure at 6.5 bar. The following feed compositions were used (O_2 to H_2 ratio of 2):

- *no* CO_2: 7.7% H_2, 15.4% O_2, 76.9% N_2
- *with* CO_2: 7.7% H_2, 15.4% O_2, 61.5% CO_2, 15.4% N_2

The tests to analyse the rate of H_2O_2 decomposition were made in batch reactor mode, starting with a solution in which already H_2O_2 was initially present (2000–3000 ppm) and sending to the reactor the same feeds reported above, except that O_2 was not present and substituted with an equal amount of N_2. In the tests with pyridine, 240 μmol of pyridine were added to methanol.

Gas analysis for H_2 and O_2 was made using a gas chromatograph (Agilent 3000A equipped with a Molsieve 5A column using Ar as carrier gas). The reaction products were analysed by potentiometric titrations of H_2O_2 (Metrohm, 794 Basic Trino) and H_2O (Metrohm, 831 KF Coulometer), respectively. The H_2O_2 selectivity is defined as follows:

$$H_2O_2 \quad \text{selectivity} \quad (\%) = \text{mol } H_2O_2/(\text{mol } H_2O_2 + \text{mol } H_2O)$$

While the H_2O_2 productivity is expressed as mg of H_2O_2 formed per mg of Pd.

3. Results and discussion

3.1. Synthesis of H_2O_2 on Pd–SiO_2 and Pd–SBA in the absence and presence of CO_2

Table 1 reports the comparison of the performances (batch reactor) of Pd–SiO_2 and Pd–SBA catalysts in the absence and presence of CO_2 in the feed. The concentration of H_2 and O_2 is the same in the two types of tests, being CO_2 substituted with N_2 in the feed. Due to the solubilization of CO_2 in the methanol and its effect in the modification of the properties, we could shortly indicate the two tests as made using methanol and CO_2-expanded methanol, respectively. Note that the total pressure in these tests is 6.5 bar and thus the conditions are quite far from those to have supercritical CO_2. The properties of CO_2-expanded solvents have been discussed in detail by Subramaniam et al. [40–43] that evidenced how the presence of CO_2 in the mixed medium increases the O_2 solubility by ca. 100 times compared to that in the neat organic solvent. Park and Yoo [44] suggested that the effect is probably related to the reaction of CO_2 with O_2 to form a reversible peroxcarbonate species ($CO_4{}^{2-}$) which increases the effective solubility of O_2 and possibly plays also additional roles. These cited studies in CO_2-expanded solvents were referring mainly to liquid phase oxidation of p-xylene to terephthalic acid.

In our case (Table 1), we observed that also in the direct synthesis of H_2O_2 a very strong increase in both the productivity and selectivity to H_2O_2 could be achieved. The productivity (after 0.2 h) increases of ca. 5 times for Pd–SiO_2 and ca. 8 times for Pd–SBA. Also the increase in the selectivity is larger for Pd–SBA. Therefore, for both catalysts the use of CO_2-expanded methanol leads to a significant increase in the performances, but the effect is enhanced in Pd–SBA.

As reported in the experimental part, there is a fast initial decrease of the pressure in the batch reactor after the stop of the feed and the starting of the mixing of the catalyst, due to the consumption of H_2 and O_2. In the tests with CO_2, the initial pressure of 6.5 bar decreases to 5.2 bar after 0.2 h and 4.5 bar after 0.4 h, to slowly further decrease later reaching a final pressure of 4.2 bar. On the contrary, without CO_2, the pressure decrease is much slower and evidences a more constant rate during the 4 h of the experiments. Therefore, after about half an hour most of the O_2 and H_2 are already consumed in the case of the tests with CO_2 and the performances for longer times are indicative of the effect of the catalyst in catalyzing the decomposition of the formed H_2O_2, i.e. the rate of synthesis of H_2O_2 significantly reduces and the consecutive decomposition of H_2O_2 may become predominant. On the contrary, due to the slower rate of H_2 and O_2 consumption without CO_2 the productivity and selectivity after 4 h are still dominated from the synthesis of H_2O_2.

With these considerations, it is possible to analyze the data in Table 1 which report together with the productivity and selectivity observed after 0.2 h also that observed after 4 h. It may be noted that in Pd–SiO_2 the productivity and selectivity after 4 h is similar, only slightly improved, with respect to that after 0.2 h. On the contrary, there is a significant decrease of both productivity and selectivity in the case of Pd–SBA. This indicates that the latter catalyst decomposes with a larger rate the formed H_2O_2 with respect to Pd–SiO_2. In the tests without CO_2, on the contrary, the productivity and selectivity of both catalysts increases in passing from 0.2 h to 4 h, suggesting that in absence of CO_2 the rate of decomposition of H_2O_2 on Pd–SBA is lower.

In the tests with and without CO_2 on both catalysts the AA analysis of the catalyst and solution after the tests indicates that a quite low amount of Pd is leached, less than 0.5 mg i.e. less than 5% of the amount present on the catalyst (Table 1). The amount is nearly independent on catalyst nature and presence of CO_2 in the feed, indicating no correlation with the catalytic behavior. After filtration of the catalyst, the solution was proven to be inactive in the

Table 1
Batch reactor tests on the effect of CO_2 in the feed on the productivity and selectivity to H_2O_2 of Pd–SiO_2 and Pd–SBA catalysts after 0.2 h and 4 h of reaction time. The leaching of Pd after 4 h of catalytic tests (mg leached and % with respect to the total Pd) is also reported.

Catalyst	Feed	Productivity, $mg_{H_2O_2}/mg_{Pd}$		Selectivity, %		Leaching, mg_{Pd} (% of Pd)
		After 0.2 h	After 4 h	After 0.2 h	After 4 h	
Pd–SiO_2	No CO_2	3.5	4.1	18	24	0.3 (4.1%)
	With CO_2	18.2	18.9	35	42	0.4 (5.5%)
Pd–SBA	No CO_2	3.4	4.3	9	18	0.2 (2.4%)
	With CO_2	27.2	23.9	57	40	0.4 (4.8%)

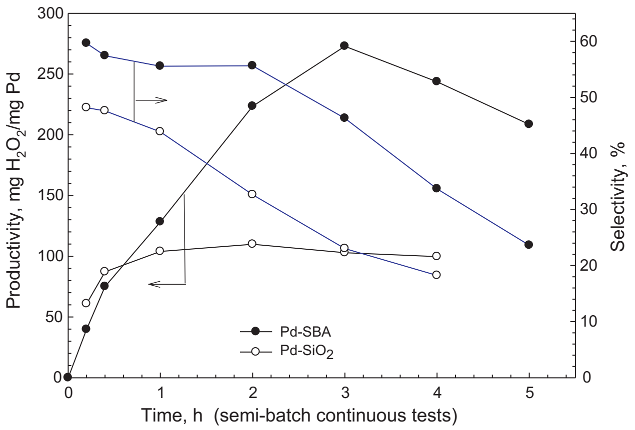

Fig. 1. Semi-batch continuous tests (6.5 bar) of the synthesis of H_2O_2 on Pd–SiO_2 and Pd–SBA catalysts.

further H_2O_2 synthesis, indicating that this small amount of leached Pd has no influence on the observed catalytic behavior.

Batch reactor tests are those used by most of the authors in studying the catalytic behavior in direct H_2O_2 synthesis, but the effective partial pressures of H_2 and O_2 may change during the reaction, as discussed above. For this reason, we have also investigated the behavior of Pd–SiO_2 and Pd–SBA catalysts in semi-batch continuous tests, were the gas phase feed composition (with CO_2) and pressure is maintained constant during the experiments. The results are reported in Fig. 1.

The initial performances of Pd–SiO_2 and Pd–SBA, e.g. in about the first 30 min of tests time, are similar, although the productivity of Pd–SiO_2 is slightly higher and the selectivity lower. Both catalysts show a productivity after 1 h of about 100–200 $mg_{H_2O_2}/mg_{Pd}$ which is quite good considering the low pressure of operation (6.5 bar), while most of the literature and patent data refer to much higher pressures (40–100 bar). Higher pressures of operation allow also a higher selectivity to H_2O_2, but the technical objective for this reaction is the possibility to obtain good catalytic performances at low pressure (e.g. below about 15–20 bar) due to cost and safety issues.

After 1 h of time on stream, however, the productivity to H_2O_2 on Pd–SiO_2 nearly stops, while a linearly increase in the case of Pd–SBA catalyst up to about 3 h of time on stream is observed, to decrease then for longer times. The selectivity to H_2O_2 decreases with the time on stream for both catalysts from the initial value of ca. 60% and 50% for Pd–SBA and Pd–SiO_2, respectively. The AA analysis of the catalyst and solution after these tests indicates that the leached Pd was 0.13 mg and 0.34 mg for Pd–SBA and Pd–SiO_2, respectively, i.e. 1.5% and 3% of the total amount of Pd in the catalyst, respectively. As commented for Table 1, the change of the catalytic behavior with time on stream cannot be attributed to this amount of leached Pd.

3.2. Decomposition of H_2O_2

The tests in the direct synthesis of H_2O_2 indicate that both Pd–SiO_2 and Pd–SBA catalysts may show a different rate of H_2O_2 decomposition which depends on the presence of CO_2 in the feed. We have thus made batch reactor tests similar to those of H_2O_2 synthesis, but starting from a solution already containing 2000–3000 ppm H_2O_2, and substituting O_2 with N_2 in the feed. In this way, H_2 which could promote the H_2O_2 hydrogenolysis, is present, but oxygen necessary for the synthesis of H_2O_2 is absent. Tests were made both in the presence and absence of CO_2 in the feed. The results are shown in Fig. 2 which reports the amount of decomposed H_2O_2 per mg_{Pd} as a function of the time.

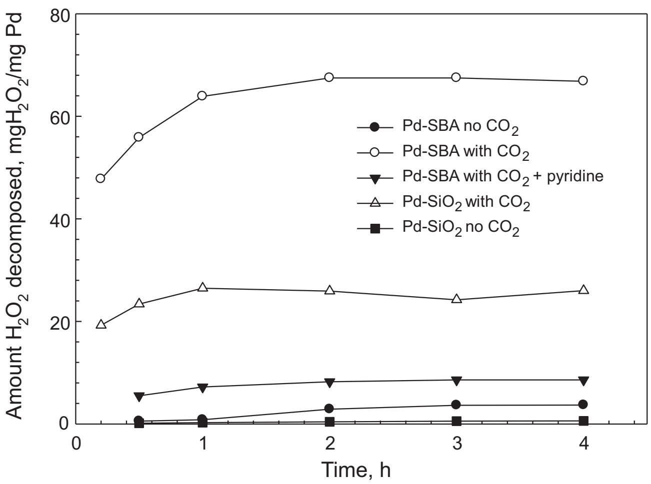

Fig. 2. Comparison of the decomposition of H_2O_2 on Pd–SiO_2 and Pd–SBA catalysts in the presence or absence of CO_2 in the $H_2/CO_2/N_2$ feed (see text). The effect of the presence of pyridine (240 μmol) in methanol solution is also reported.

Both catalysts show a very low activity in H_2O_2 decomposition in the absence of CO_2, and a significant increase when CO_2 is present in the feed. The effect, however, is significantly larger for Pd–SBA. The effect could be related to a change of the acidity of the solution in passing from methanol to CO_2-expanded methanol. In water, the optimal stability and rate of H_2O_2 synthesis was shown ca. in the 3–4 pH range. At higher pHs, the decomposition of H_2O_2 becomes relevant. Although we use anhydrous methanol as the solvent, water is present in solution being a reaction product and being present in traces in the gas feed sent to the reactor. Both catalysts have a hydrophilic character, and thus water probably remain adsorbed on them, particularly in micropores or SBA-15 channels. Therefore, it is not unlikely that in presence of CO_2 in the feed a change in the pH of this adsorbed water occurs and this determines the enhanced rate of decomposition of H_2O_2. This could also explain why the selectivity to H_2O_2 decreases with time on stream (Fig. 1), being increasing the amount of water in solution.

In order to check whether the presence of weak silanol groups could be responsible for the decomposition of H_2O_2, we have also tested the decomposition of H_2O_2 in the presence of little amounts of pyridine to block the activity of these silanol groups. The amount of added pyridine was about equivalent to the amount of silanol groups in SBA-15 which could be estimated from FT-IR data [39].

In the presence of pyridine, the decomposition rate of H_2O_2 on Pd–SBA (tests with CO_2) is strongly depressed, suggesting that weak silanol groups could be responsible for this reaction. However, pyridine may also have a different effect related to the chemisorption on Pd metal particles which could inhibit H_2 adsorption and thus H_2O_2 hydrogenolysis rate. In a previous work Grassian and Muetterties [45] found a interaction of pyridine with Pt (1 1 1) at low temperature and it was observed by other authors [46–47].

To analyze this aspect, the synthesis of H_2O_2 in a batch reactor test in the presence or absence of pyridine in solution was investigated using CO_2 in the feed and Pd–SBA catalyst. The results are reported in Fig. 3 (productivity and selectivity to H_2O_2, Fig. 3a and b, respectively).

Pyridine, even if present in small amounts, strongly depresses the synthesis of H_2O_2 on Pd–SBA in the presence of CO_2 in the feed. Both productivity (Fig. 3a) and selectivity (Fig. 3b) are significantly decreased. Therefore, pyridine strongly chemisorbs on the Pd surface inhibiting its reactivity. It is thus not possible to clearly discriminate whether the enhanced rate of H_2O_2 decomposition in the presence of CO_2 is due to the activity of weak acid groups of

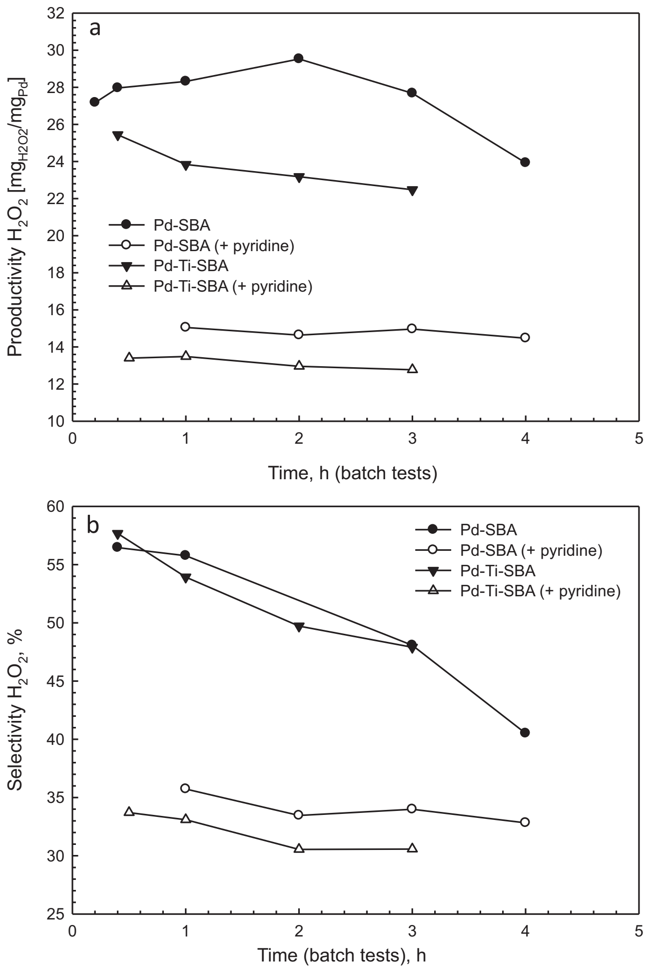

Fig. 3. Effect of pyridine (240 μmol) on the synthesis of H_2O_2 in batch reactor. Tests with CO_2 on Pd–SBA and Pd–Ti–SBA catalysts. Productivity and selectivity to H_2O_2: Fig. 3a and b, respectively.

the support (silanol groups) or to the hydrogenolysis over the Pd surface.

In order to better understand this aspect, we have investigated the effect of pyridine on both the decomposition and synthesis of H_2O_2 in the presence of CO_2 using Pd–Ti–SBA as the catalyst. The results are reported in Table 2 and Fig. 3 in comparison with Pd–SBA catalyst. As discussed in a more detail elsewhere [37,39], the grafting of Ti on SBA-15 leads to a reconstruction of the inner walls of SBA-15 channels with a decrease of the amount of silanol groups. Therefore, the comparison between Pd–SBA and Pd–Ti–SBA could give an indication on the role of silanol groups present inside the channels of SBA-15 for the synthesis and decomposition of H_2O_2.

Table 2
Batch reactor tests on the decomposition of H_2O_2 on Pd–SBA and Pd–Ti–SBA catalysts.

Feed/solution	Amount of H_2O_2 decomposed, $mg_{H_2O_2}/mg_{Pd}$			
	Pd–SBA		Pd–Ti–SBA	
	After 0.5 h	After 3 h	After 0.5 h	After 3 h
No CO_2/methanol	0.55	3.64	3.57	8.47
With CO_2/methanol	55.85	67.47	31.33	33.10
With CO_2/methanol + pyridine	5.51	8.60	26.47	29.01

For the synthesis of H_2O_2, Pd–Ti–SBA shows a slightly lower productivity with respect to Pd–SBA (Fig. 3a), nevertheless a similar trend of decreasing productivity for the longer times of reaction is observed. The selectivity to H_2O_2 is similar (Fig. 3b). The effect of pyridine is nearly the same on the two catalysts.

In the decomposition of H_2O_2 (Table 2) both catalysts show an enhanced rate in the presence of CO_2, but the rate of decomposition on Pd–Ti–SBA is nearly the half of that on Pd–SBA. In addition, the decomposition rate is strongly depressed on Pd–SBA in the presence of pyridine in solution, while the effect is much less relevant in the case of Pd–Ti–SBA sample.

These results thus evidence that both the presence of weak acid silanol groups and the hydrogenolysis on Pd surface contribute to the decomposition of H_2O_2 and are both enhanced in the presence of CO_2 in the feed. While no great differences were observed on the reactivity, when the supports are used without Pd. Pyridine in small amounts in solution suppresses both reactions, but also the synthesis of H_2O_2 and thus this is not an effective method to improve the catalytic performances.

3.3. *Characterization of the catalysts before and after use*

The wide-angle X-ray diffraction (XRD) patterns of Pd–SiO_2 and Pd–SBA fresh samples in the 20–80 2θ region are reported in Fig. 4a. In Pd–SiO_2, besides to the very broad band centred to ca. 23° due to amorphous silica, only a weak and broad band at about 34° due to PdO could be observed. In Pd–SBA instead this band is more

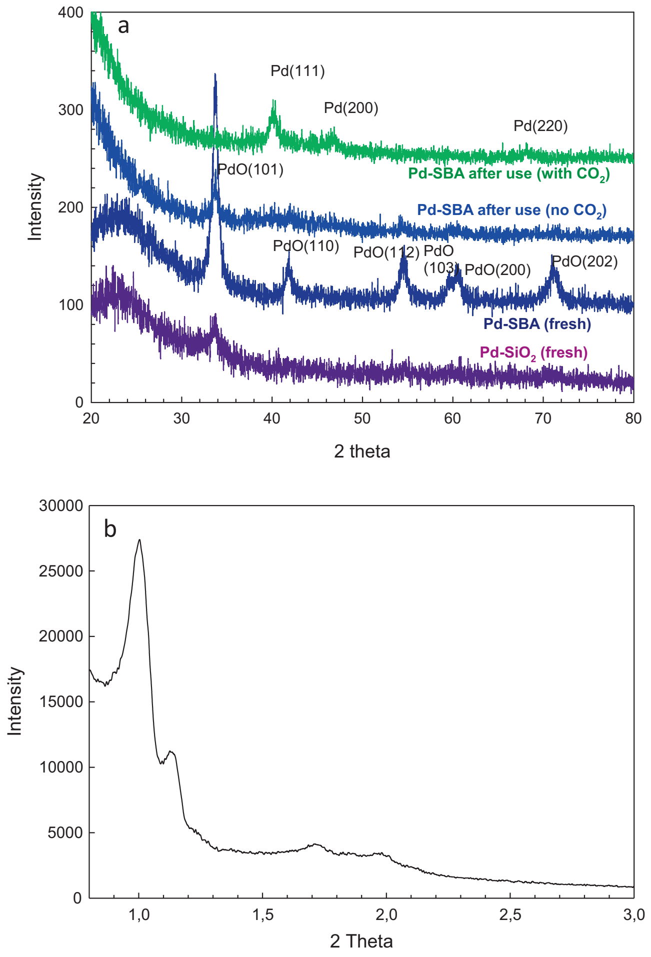

Fig. 4. (a) Wide-angle XRD pattern of fresh Pd–SiO_2 and Pd–SBA samples, and of Pd–SBA after use in direct H_2O_2 synthesis in the absence or presence of CO_2. (b) Small-angle XRD pattern of fresh Pd–SBA sample.

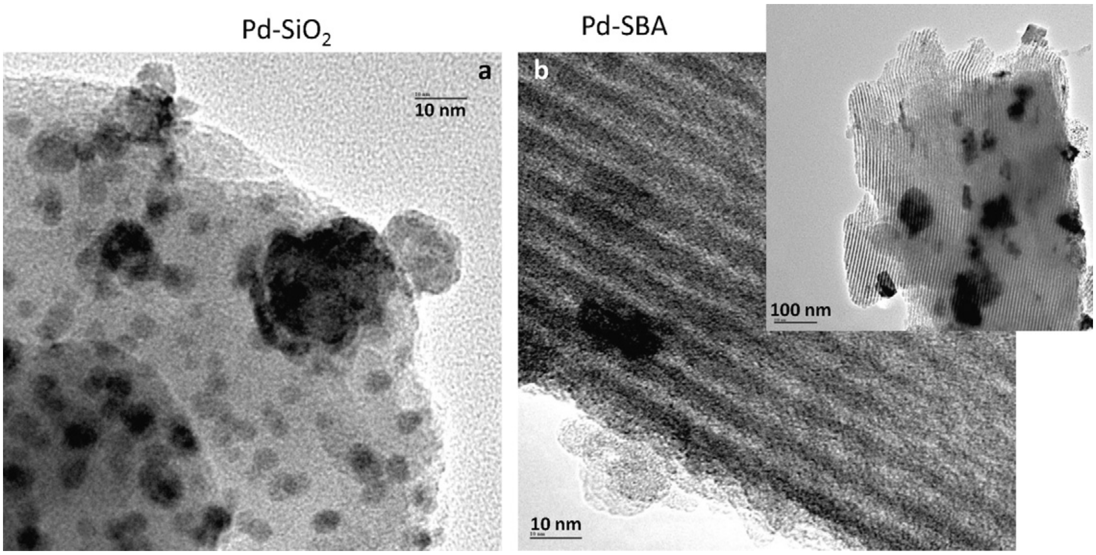

Fig. 5. TEM images of fresh Pd–SiO_2 (a) and Pd–SBA (b) samples.

intense, even if also rather broad, and also the other PdO diffraction lines could be evidenced. Fig. 4b reports for Pd–SBA the small-angle X-ray scattering. At low angle, peaks at ca. 0.95°, 1.20° and two smaller peaks at ca. 1.65° and 1.90° characteristic of the reflections of hexagonal mesoporous SBA-15 are present, indicating the presence of channels with a good mesoscopic order. No diffraction lines are instead present in the Pd–SiO_2 sample which do not show this mesoscopic order.

After use with CO_2, there is a significant decrease in the intensity of PdO diffraction lines (Fig. 4a). In Pd–SBA only the PdO(1 0 1) could be evidenced, while no reflections could be seen in Pd–SiO_2 (omitted for clarity). After use with CO_2, instead that PdO reflections completely disappear in Pd–SBA, but new weak and broad reflections due to metallic Pd could be observed. In the case of Pd–SiO_2, instead again no reflections could be seen (omitted for clarity). No change in the small-angle X-ray scattering region of Pd–SBA could be instead observed after the catalytic tests.

Therefore, XRD data evidence that there is a modification of the nature of Pd particles during the reaction and that the modification depends on the use or not of the CO_2-expanded solvent.

Fig. 5 reports the transmission electron microscopy (TEM) images of fresh Pd–SiO_2 (a) and Pd–SBA (b) samples. In Pd–SiO_2, well-distributed round-shaped Pd particles with mean diameter in the 3–6 nm range are found together with some larger aggregates of these Pd particles. In Pd–SBA, the presence of the ordered channels could clearly evidenced, but without Pd particles located inside the channels. The Pd is present as large particles or aggregates of these particles deposited on the external surface of the SBA-15 crystallites.

Fig. 6a reports the TEM images of the Pd–SBA sample after catalytic tests with or without CO_2. It could be clearly seen that there is a change in the arrangement of Pd particles, which in part also enter inside the channels with the formation of few distinct particles (with average diameter 4 nm) together with elongated 1D-type particles with diameter corresponding to that of the SBA-15 channels (about 5–6 nm) and length up to over 50 nm. The effect is particularly evident after use with CO_2. Together with these Pd particles inside the channels, some large particles on the outside surface of SBA-15 crystallites are present.

Fig. 6b reports TEM images of Pd–SBA after the tests in H_2O_2 decomposition in the absence of CO_2, where the migration of Pd inside the channels with formation in some case of elongated particles is also observed. This result evidences that CO_2-expanded methanol is not necessary, although facilitates the migration of Pd inside the channels. The presence of H_2 and probably of H_2O_2 is instead necessary, because no appreciable change was observed in Pd–SBA sample put in methanol solution.

Therefore, relatively large PdO particles are present in the fresh samples, but during the reaction, due to the reduction and reoxidation, there is a migration of Pd inside the SBA-15 channels with the formation of elongated Pd particles together with few distinct round-shaped particles. The presence of CO_2, enhancing the solubility of probably both O_2 and H_2, facilitates this mechanism of relocation of Pd. As evidenced in Fig. 6a, probably the channels access by the reactants could be limited, when these elongated particles form.

Based on these indications, we could tentatively interpret the results reported in Fig. 1. The initial activity of the catalyst is high due to the presence of PdO particles which are however progressively reduced during the reaction decreasing the productivity and probably the selectivity, being enhanced the rate of H_2O_2 hydrogenolysis.

In Pd–SiO_2, due to the initial better dispersion, the initial activity is higher. However, in Pd–SBA there is an additional mechanism of relocalization of Pd with an initial migration inside the ordered channels, where probably it is more thermodynamically stable. This causes an increase in the number of Pd particles with a consequent compensation of the lowering of the activity due to the reduction of Pd particles. Therefore, the productivity in Pd–SBA continues to increase with time on stream differently from Pd–SiO_2. However, for the longer times, due to probably a blocking of the reactants diffusion inside the channels when larger elongated Pd particles form, there is a decrease of the number of accessible Pd particles which determines the decrease of the productivity at the longer times on stream (Fig. 1).

The presence of an ordered mesopore structure is thus beneficial for the initial relocation of Pd and formation of smaller particles inside the channels, but their high mobility, particularly in the tests in the presence of CO_2, causes their aggregation and partial occlusion of the channels. In addition, as discussed before, the presence of even weak acidity due to silanol groups determines an enhancement in the rate of the consecutive decomposition of H_2O_2.

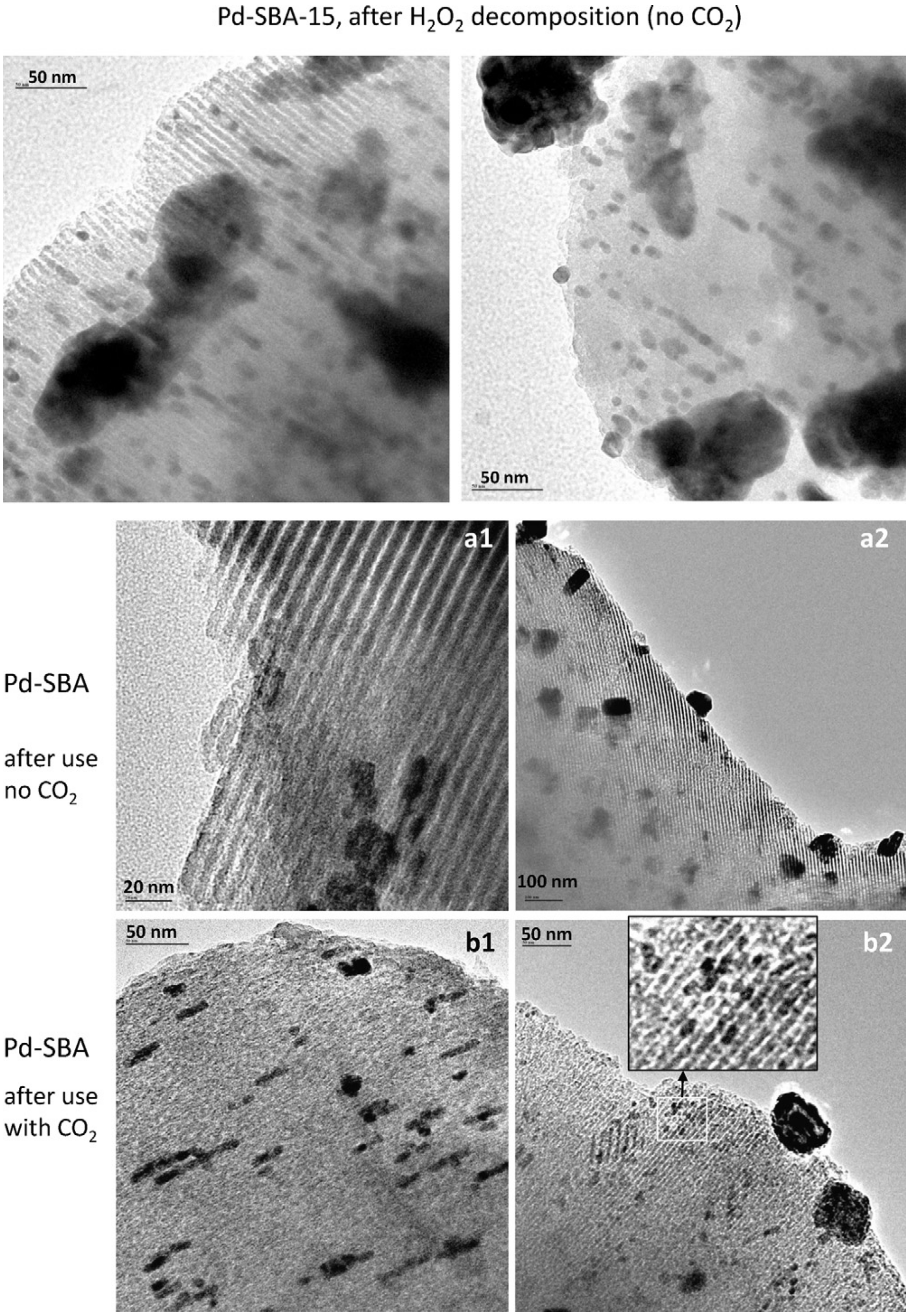

Fig. 6. (a) TEM images of Pd–SBA after the catalytic tests in H_2O_2 synthesis in the absence (a1 and a2) and presence (b1 and b2) of CO_2 in the feed. (b) TEM images of Pd–SBA after the catalytic tests in H_2O_2 decomposition in the absence of CO_2 in the feed.

4. Conclusions

The use of CO_2-expanded methanol leads to a significant increase in the rate of H_2O_2 synthesis for both Pd–SiO_2 and Pd–SBA samples, especially in the latter. The effect derives from an increased solubility of H_2 and O_2 which increases the reaction rate, but also determines a relocation of Pd particles which migrates inside the mesopores of SBA-15. For longer times of reaction, elongated Pd particles form which probably partially inhibit the reactant diffusion. This determines a decrease of the productivity which, however, at the maximum is about 2.5 times higher than that of the analogous Pd–SiO_2 sample in semi-batch continuous tests.

The use of CO_2-expanded methanol leads also to an enhanced rate of H_2O_2 decomposition, particularly in the Pd–SBA sample, where together with the H_2O_2 hydrogenolysis, an additional path due to H_2O_2 decomposition catalyzed by weak acid groups (silanols) is present. The addition of pyridine to the solution strongly inhibits both reactions, but also the synthesis of H_2O_2 due probably to the strong chemisorption over the Pd particles. The grafting with Ti of the inner walls of SBA-15 channels in order to decrease the amount of silanol groups has a positive effect to control the decomposition of H_2O_2 catalyzed by these groups.

Acknowledgements

This contribution was realized in the frame of the activities of the Network of Excellence IDECAT (NMP3-CT2005-011730, Integrated Design of Catalytic Nanomaterials for a Sustainable Production) and of the national PRIN projects which are gratefully acknowledged. Within the IDECAT project, the collaboration with the Fritz-Haber Institut der Max Plank Gesell. (Berlin, Germany) and particularly with Dr. D. Su and Prof. R. Schlögl, is acknowledged, especially for some of the TEM measurements. Technical assistance of Mr. D. Cosio (Univ. Messina, Italy) in the construction of the autoclave and related apparatus is also acknowledged.

References

[1] F. Cavani, G. Centi, S. Perathoner, F. Trifirò, Sustainable Industrial Chemistry – Principles Tools and Industrial Examples, Wiley-VCH, Weinheim, Germany, 2009.
[2] G. Blanco-Brieva, M.C. Capel-Sanchez, M.P. De Frutos, A. Padilla-Polo, J.M. Campos-Martin, J.L.G. Fierro, Ind. Eng. Chem. Res. 47 (21) (2008) 8011.
[3] G. Centi, S. Perathoner, Catal. Today 143 (1–2) (2009) 145.
[4] C. Samanta, Appl. Catal. A: Gen. 350 (2) (2008) 133.
[5] G. Centi, S. Perathoner, S. Abate, in: N. Mizuno (Ed.), Modern Heterogeneous Oxidation Catalysis, Wiley-VCH, Weinheim, Germany, 2009, p. 253.
[6] J.M. Campos-Martin, G. Blanco-Brieva, J.L.G. Fierro, Angew. Chem. 45 (42) (2006) 6962.
[7] F. Menegazzo, M. Signoretto, M. Manzoli, F. Boccuzzi, G. Cruciani, F. Pinna, G. Strukul, J. Catal. 268 (1) (2009) 122.
[8] G. Bernardotto, F. Menegazzo, F. Pinna, M. Signoretto, G. Cruciani, G. Strukul, Appl. Catal. A: Gen. 358 (2) (2009) 129.
[9] Q. Liu, J.C. Bauer, R.E. Schaak, J.H. Lunsford, Appl. Catal. A: Gen. 339 (2) (2008) 130.
[10] J.K. Edwards, B. Solsona, E. Ntainjua N., A.F. Carley, A.A. Herzing, C.J. Kiely, G.J. Hutchings, Science 323 (5917) (2009) 1037.
[11] A.A. Herzing, A.F. Carley, J.K. Edwards, G.J. Hutchings, C.J. Kiely, Chem. Mater. 20 (4) (2008) 1492.
[12] J.C Pritchard, Q. He, E.N. Ntainjua, M. Piccinini, J.K. Edwards, A.A. Herzing, A.F. Carley, J.A. Moulijn, C.J. Kiely, G.J. Hutchings, Green Chem. 12 (5) (2010) 915.
[13] J.K. Edwards, N.N. Edwin, A.F. Carley, A.A. Herzing, C.J. Kiely, G.J. Hutchings, Angew. Chem. 48 (45) (2009) 8512.
[14] Y. Nomura, T. Ishihara, Y. Hata, K. Kitawaki, K. Kaneko, H. Matsumoto, ChemSusChem 1 (7) (2008) 619.
[15] A. Staykov, T. Kamachi, T. Ishihara, K. Yoshizawa, J. Phys. Chem. C 112 (49) (2008) 19501.
[16] H.C. Ham, G.S. Hwang, J. Han, S.W. Nam, T.H. Lim, J. Phys. Chem. C 113 (30) (2009) 12943.
[17] V.R. Choudhary, C. Samanta, J. Catal. 238 (2006) 28.
[18] S. Melada, R. Rioda, F. Menegazzo, F. Pinna, G. Strukul, J. Catal. 239 (2006) 422.
[19] R. Burch, P.R. Ellis, Appl. Catal. B: Environ. 42 (2003) 203.
[20] M. Sun, J. Zhang, Q. Zhang, Y. Wang, H. Wan, Chem. Commun. 34 (2009) 5174.
[21] Q. Liu, K.K. Gath, J.C. Bauer, E.E. Schaak, J.H. Lunsford, Catal. Lett. 132 (3–4) (2009) 342.
[22] G. Blanco-Brieva, M. Pilar de Frutos Escrig, J.M. Campos-Martin, J.L.G. Fierro, Green Chem. (2010), doi:10.1039/c003700a.
[23] B. Hu, Q. Zhang, Y. Wang, Chem. Lett. 38 (3) (2009) 256.
[24] J.K. Edwards, A.F. Carley, A.A. Herzing, C.J. Kiely, G.J. Hutchings, Faraday Discuss. 138 (Nanoalloys) (2008) 225.
[25] G. Blanco-Brieva, E. Cano-Serrano, J.M. Campos-Martin, J.L.G. Fierro, Chem. Commun. (2004) 1184.
[26] C. Burato, P. Centomo, M. Rizzoli, A. Biffis, S. Campestrini, B. Corain, Adv. Synth. Catal. 348 (2006) 255.
[27] S. Abate, R. Arrigo, M.E. Schuster, S. Perathoner, G. Centi, A. Villa, D. Su, R. Schlögl, Catal. Today 157 (2010) 280–285.
[28] H.-Q. An, G.-Y. Wang, Y.J. Wang, X.-Q. Zhao, Chin. J. Inorg. Chem. 26 (3) (2010) 405.
[29] K. Mori, Y. Miura, S. Shironita, H. Yamashita, Langmuir 25 (18) (2009) 11180.
[30] K. Mori, T. Araki, S. Shironita, J. Sonoda, H. Yamashita, Catal. Lett. 131 (3–4) (2009) 337.
[31] S. Abate, G. Centi, S. Perathoner, S. Melada, F. Pinna, G. Strukul, Top. Catal. 38 (1–3) (2006) 181.
[32] S. Melada, F. Pinna, G. Strukul, S. Perathoner, G. Centi, J. Catal. 237 (2) (2006) 213.
[33] V.R. Choudhary, P. Jana, Catal. Commun. 9 (14) (2008) 2371.
[34] V.R. Choudhary, P. Jana, Appl. Catal. A: Gen. 352 (1–2) (2009) 35.
[35] S. Abate, K. Barbera, P. Lanzafame, S. Perathoner, G. Centi, Prep. Pap. -Am. Chem. Soc., Div. Pet. Chem. 53 (1) (2008) 227.
[36] T. Moreno, J. García-Serna, M.J. Cocero, Green Chem. 12 (2) (2010) 282.
[37] S. Perathoner, P. Lanzafame, R. Passalacqua, G. Centi, R. Schlögl, D.S. Su, Micropor. Mesopor. Mater. 90 (2006) 347.
[38] D. Zhao, J. Sun, Q. Li, G.D. Stucky, Chem. Mater. 12 (2000) 275.
[39] S. Perathoner, P. Lanzafame, G. Centi, F.C. Jentoft, T.V. Venkov, R. Schlögl, Stud. Surf. Sci. Catal. 170 (Part 2) (2007) 1788.
[40] M. Wei, G.T. Musie, D.H. Busch, B. Subramaniam, J. Am. Chem. Soc. 124 (11) (2002) 2513.
[41] Y. Houndonougbo, H. Jin, B. Rajagopalan, K. Wong, K. Kuczera, B. Subramaniam, B. Laird, J. Phys. Chem. B 110 (26) (2006) 13195.
[42] B. Kerler, R.E. Robinson, A.S. Borovik, B. Subramaniam, Appl. Catal. B: Environ. 49 (2) (2004) 91.
[43] X. Zuo, F. Niu, K. Snavely, B. Subramaniam, D.H. Busch, Green Chem. 12 (2010) 260.
[44] S.-E. Park, J.S. Yoo, Stud. Surf. Sci. Catal. 153 (2004) 303.
[45] V.H. Grassian, E.L. Muetterties, J. Phys. Chem. 90 (1986) 5900.
[46] W. Erley, R. Xu, C.J. Hemminger, Surf. Sci. 389 (1997) 272.
[47] T.S. Nunney, J.J. Birtill, R. Raval, Surf. Sci. 427–428 (1999) 282.